

AperTO - Archivio Istituzionale Open Access dell'Università di Torino

Chemical stability and dehydration behavior of a sepiolite/indigo Maya Blue pigment

This is the author's manuscript

Original Citation:

Availability:

This version is available <http://hdl.handle.net/2318/86686> since

Published version:

DOI:10.1016/j.clay.2011.01.027

Terms of use:

Open Access

Anyone can freely access the full text of works made available as "Open Access". Works made available under a Creative Commons license can be used according to the terms and conditions of said license. Use of all other works requires consent of the right holder (author or publisher) if not exempted from copyright protection by the applicable law.

(Article begins on next page)



UNIVERSITÀ DEGLI STUDI DI TORINO

This Accepted Author Manuscript (AAM) is copyrighted and published by Elsevier. It is posted here by agreement between Elsevier and the University of Turin. Changes resulting from the publishing process - such as editing, corrections, structural formatting, and other quality control mechanisms - may not be reflected in this version of the text. The definitive version of the text was subsequently published in **/Chemical stability and dehydration behavior of a sepiolite/indigo Maya Blue pigment**, *Applied Clay Science* 52, 2011, [10.1016/j.clay.2011.01.027](https://doi.org/10.1016/j.clay.2011.01.027)].

You may download, copy and otherwise use the AAM for non-commercial purposes provided that your license is limited by the following restrictions:

(1) You may use this AAM for non-commercial purposes only under the terms of the CC-BY-NC-ND license.

(2) The integrity of the work and identification of the author, copyright owner, and publisher must be preserved in any copy.

(3) You must attribute this AAM in the following format: Creative Commons BY-NC-ND license (<http://creativecommons.org/licenses/by-nc-nd/4.0/deed.en>), [[10.1016/j.clay.2011.01.027](https://doi.org/10.1016/j.clay.2011.01.027)]

Chemical stability and dehydration behavior of a sepiolite/indigo Maya Blue pigment

R. Giustetto^{*a,c}, O. Wahyudi^a, I. Corazzari^{b,c,d}, F. Turci^{b,c,d}

^a *Dip. di Scienze Mineralogiche e Petrologiche – Università degli Studi di Torino*

Via Valperga Caluso 35, 10125 Torino (Italy)

^b *Dip. di Chimica I.F.M. – Università degli Studi di Torino*

Via Pietro Giuria 7, 10125 Torino (Italy)

^c *Nanostructured Interfaces and Surfaces (NIS) – Centre of Excellence*

Via Pietro Giuria 7, 10125 Torino (Italy)

^d *Interdepartmental Centre “G. Scansetti” for Studies on Asbestos and other Toxic particulates*

via Pietro Giuria 7, 10125 Torino (Italy)

*Corresponding author. E-mail address: roberto.giustetto@unito.it. Tel.: +390116705122; Fax: +390116705128

Abstract

Sepiolite is a fibrous clay mineral which, together with palygorskite, is an end-member of the palygorskite-sepiolite polysomatic series. Both palygorskite and sepiolite are renowned in Cultural Heritage studies because when properly complexed to the indigo dye they form Maya Blue, a synthetic blue pigment used in Pre-Columbian America which is famous for its exceptional stability. Freshly-synthesized Maya Blue-like composites can be prepared by grinding and heating such clays with indigo. The pigment can be considered a precursor of modern inclusion compounds, with indigo molecules possibly being hosted within nano-tunnels crossing the clay frameworks, usually filled by loosely-bound zeolitic H₂O and tightly-bound structural OH₂. While the palygorskite/indigo composite has been widely studied, few papers have been focused on the analogous sepiolite-based adduct. An in-depth research was therefore planned in order to characterize the composite structural features when indigo is hosted on the sepiolite matrix, whose importance may be relevant to both the Cultural Heritage and Materials

Science fields. A Maya Blue-alike composite was obtained by properly mixing and heating (190°C) pure sepiolite with a 2 wt% synthetic indigo. SEM-EDS analysis showed the clay crystal-chemical formula to be coherent with the ideal one. Performed stability tests proved the resistance of the synthesized sepiolite + indigo pigment to be lower than the one typical of palygorskite + indigo adducts. Concentrated HNO₃ progressively decolorized and completely destroyed the pigment structure, due to a more pronounced intrinsic fragility of the sepiolite framework compared to palygorskite. Prolonged NaOH attack did not substantially alter the pigment colour but caused the hosting matrix to undergo a progressive phase transformation from sepiolite to loughlinite, a similar clay mineral with intra-framework Na ions. Such a transition is favoured by indigo, whose exact role has yet to be understood. Conventional thermograms recorded for both pure sepiolite and the sepiolite + indigo composite gave indirect evidence about the encapsulation of the dye within the tunnels, as the total amount of zeolitic H₂O decreased in the pigment due to the channels volume being partly occupied by indigo. Thermogravimetry coupled with gas chromatography and mass spectrometry proved that organic splinters related to fragmentation of the adsorbed indigo molecules leave the hosting matrix in the 300-500°C temperature interval. As loss of indigo and OH₂ proceeded simultaneously, it is legitimate to suppose that H-bonds may form within the clay channels between Mg-coordinated OH₂ and the dye C=O/N-H groups, thus conferring to the pigment its renowned stability.

Keywords: sepiolite, indigo, Maya Blue, stability, TGA-GC-MS analysis.

1. Introduction

Sepiolite (ideal formula: Mg₈Si₁₂O₃₀(OH)₄(OH₂)₄•nH₂O; n ≤ 8) is a natural occurring phyllosilicate clay with fibrous morphology, found in a wide variety of geological environments

and mined for centuries due to its useful properties. The name sepiolite was first used by Glocker (1847) and is derived from the Greek term for cuttlefish, whose bone is as light and porous as the mineral itself. Another term still used is *Meerschaum*, coined by Kirwan (1794; in Mackenzie, 1963). Over 90% of sepiolite is mined in Spain (Miocene deposits), with an annual production of around 800 thousand tons (O'Driscoll, 1992). Small productions are located in Nevada (USA), Turkey and China. Natural occurrences of sepiolite are often found in association with other clay and non-clay minerals, such as carbonates, quartz, feldspar and phosphates.

Sepiolite, together with palygorskite, is an end-member of the palygorskite/sepiolite polysomatic series which include several intermediate members such as kalifersite (Ferraris et al., 1998), falcondoite (Springer, 1976), loughlinite (Fahey et al., 1960), yofortierite (Perrault et al., 1975) and taperssuatsiaite (Camara et al., 2002). In both sepiolite and palygorskite the strain between the octahedral and tetrahedral sheets causes the former to split into ribbons elongated in the Z-axis direction, whereas the latter preserves its continuity by means of an inversion in the orientation of the tetrahedral apexes, forming alternate bonds with the upper or lower octahedral ribbon. The structure of these clay minerals may also be described as modulated TOT silicate layers showing a waving T sheet and a discontinuous O sheet (Guggenheim and Eggleton, 1988) or as a framework of chessboard connected TOT ribbons (Ferraris et al., 2008).

The structure of sepiolite was proposed independently by Nagy and Bradley (1955) and Brauner and Preisinger (1956) and recently refined by Post et al. (2007) using the Rietveld method on synchrotron diffraction patterns. Sepiolite is a microporous clay mineral whose framework is crossed by microchannels elongated in the [001] direction, usually filled by weakly-bound zeolitic H₂O and sometimes exchangeable cations (to ensure electric neutrality). Tightly-bound, structural OH₂ molecules complete the coordination of octahedral cations (Mg) at the ribbon borders. The dimensions of the TOT ribbons and microchannels may vary as in palygorskite the

former include two pyroxene-like tetrahedral chains, elongated in the [001] direction and enclosing five octahedral sites, whereas in sepiolite the TOT strips consist of three pyroxene-like tetrahedral chains, sandwiching a Mg–(O;OH) octahedral strip (Fig. 1). As a consequence, the maximum effective width¹ of the channels is wider in sepiolite (10.6 x 3.7 Å) than in palygorskite (6.4 x 3.7 Å).

(INSERT FIGURE 1)

Sepiolite has a broad variety of useful properties and applications, due to its characteristic microporosity and high surface area. It is mostly used for sorptive applications, since it can retain up to 250% of its own weight in water located in the channels or bonded to the surface. Sepiolite is also widely used as a decolorizing agent, being able to seize colored particles or dyes during filtration or percolation (Shariatmadari et al., 1999; Rytwo et al., 2000; Alkan et al, 2004; Özdemir et al., 2006; Dogan et al., 2007; Alkan et al, 2007). Thermal treatment (activation: 200° C), extrusion and acid treatment usually enhance such capability (Jones and Galan, 1988). Another fundamental use is that of a carrier, achieved through impregnation of catalytically important ions (such as Ni²⁺, Ptⁿ⁺, Pdⁿ⁺, Zn²⁺, Co²⁺ and Cu²⁺) on the clay surface and substitution with octahedral Mg²⁺ cations. Catalytic processes achieved are dehydration, hydrogenation, dehydrogenation, desulfuration and various hydrocracking processes (Damyanova et al., 1996; Shimizu et al., 2004; Martín and Melo, 2006). Other applications include the synthesis of organo-mineral derivatives, modification of rheological properties and as a reinforcing filler in rubbers and plastic.

Palygorskite and sepiolite are well known in the Cultural Heritage field since both clays are generally reputed to be essential components of one of the most famous and studied pigments: the so-called Maya Blue. Used by the ancient Mayas in pre-Columbian America from the VI to

¹The effective width is defined as the smallest free aperture across the channel, obtained by subtracting the ionic radius of oxygen from the O–O distance measured between both sides of the channel (McCusker, 2005).

the XVII century A.D., Maya Blue can be found in mural paintings and to decorate statues and pottery. The pigment had also a strong symbolic meaning: prisoners to be sacrificed to Mayan gods had their skin completely painted in blue (Reyes-Valerio, 1993; Arnold et al., 2008). It is nowadays commonly accepted that Maya Blue is the result of an indissoluble association between a clay – mostly palygorskite – and an organic dye – indigo ($C_{16}H_{10}N_2O_2$). Many archaeological specimens, however, were found to contain palygorskite/sepiolite mixtures whereas others contained only sepiolite (Gettens, 1962; De Yta, 1976; Reyes-Valerio, 1993; Giustetto, 2003). From its re-discovery in modern times (Merwin, 1931), Maya Blue soon captured the attention of the scientific community due to its exceptional chemical stability: the pigment is virtually unaltered by the attack of acids, alkalis or solvents and does not fade when exposed to light.

The procedure for the pigment preparation is described in the literature, whether using raw precursors and methods (presumably adopted by ancient Mayas: Reyes-Valerio, 1993) or unpolluted ingredients and laboratory techniques (Van Olphen, 1966; Kleber et al., 1967; Polette-Niewold et al., 2007). Maya Blue is obtained by mixing and grinding in proper quantities the clays (palygorskite or sepiolite) with indigo (usually no more than 2 wt.%) and heating up to 120–190° C for several hours. Heating is fundamental to achieve stability: an unheated palygorskite/indigo mixture, although similar in aspect to Maya Blue, is completely discolored when attacked with HNO_3 . According to the most quoted hypothesis heating causes a progressive loss, albeit incomplete, of the zeolitic H_2O (Jones and Galan, 1988) thus allowing the diffusion of indigo within the partially emptied nano-tunnels. The penetration of indigo inside the clay micropores is stabilized through the formation of chemical bonds between the clay and the dye, which keep *in situ* the guest molecules thus conferring the pigment its resistance. Though widely studied, the real nature of the established interactions between indigo and the hosting clay (mainly palygorskite) is still disputed, whether H-bonds formed within the channels (Chiari et al., 2003; Fois et al., 2003; Reinen et al., 2004; Giustetto et al., 2005;

Giustetto et al., 2006) or carbonyl-silanol and metal-oxygen interactions occurring on the clay surface (Hubbard et al., 2003; Polette-Niewold et al., 2007; Manciu et al., 2008). Whatever the source, these interactions guarantee the pigment stability and resistance to severe chemical attack. The ancient blue pigment created by Mayas can therefore be considered a forerunner of the modern inclusion compounds, in which an inorganic “host” framework can accommodate a “guest” molecule into cages or channels.

As most studies have been focused so far on characterization of the structure and host/guest interactions in a palygorskite-based Maya Blue pigment, new in-depth research was planned in order to investigate the very same features when fixation of indigo occurs on the sepiolite matrix. As stated above, the presence of sepiolite in original Maya Blue specimens, though less recurrent than palygorskite, is well documented in the literature (Gettens, 1962; De Yta, 1976; Reyes-Valerio, 1993). In addition, Van Olphen (1966) showed that stable synthetic pigments can be prepared by mixing and heating sepiolite with indigo, whereas the use of other lamellar clays (montmorillonite, illite and nontronite) brings no consistent result. Despite their renowned similarities, however, the structural differences between palygorskite and sepiolite might cause the mutual interactions with the guest indigo dye to have peculiar features typical for each clay. Based on these premises, an exhaustive characterization of the sepiolite-based composite with indigo may be fundamental to not only the Cultural Heritage, but also the Materials Science field, as it is well known that analogous host/guest adducts may find application in a wide range of possible uses (pigment, paints, polymer reinforcements, control release, carriers and optics) (Calzaferri et al., 2003; Brühwiler et al., 2009; Giulieri et al., 2009).

2. Materials and experimental

Particular care was adopted in the choice of the materials to be studied. The analysis of original Maya Blue specimens made of pure sepiolite + indigo, although appealing, was excluded from the very start due to several reasons:

- i) Samples scratched from mural paintings in archaeological sites generally contain a mixture of different clays. Pure sepiolite specimens are very rare. Generally, palygorskite occurs (often as the dominant clay) but frequently lamellar clays such as nontronite, vermiculite and montmorillonite can also be present.
- ii) Authentic Maya Blue specimens are not pure. No matter how scrupulous the sample collection might be, fragments of the lower substratum (i.e. plaster) will eventually contaminate the pictorial pellicle. The high crystallinity of the polluting minerals (calcite and quartz) causes the related diffraction maxima to dominate in the XRPD patterns.
- iii) Archaeological Maya Blue specimens are not easily disposable and – forcibly – scarce in quantity. Rightly, Mexican authorities are not so willing to allow anyone to impoverish their archaeological heritage.

The current study was therefore performed on freshly-synthesized sepiolite + indigo adducts, a procedure already adopted in previous work (Hubbard et al., 2003). Natural sepiolite and synthetic indigo were provided by Sigma-Aldrich (code nos. 70253 and 56980 respectively). Natural palygorskite from the mine of Lorenzo Pech, a few kilometers from Ticul (Chapas, Mexico), was also used.

Chemical characterization was performed by electron probe microanalysis (EPMA) using a SEM Stereoscan 360, Cambridge Instrument, equipped with EDS Link Pentafet, Oxford instrument. Due to the difficulties in analyzing fibrous samples, punctual analysis were collected in different areas of a pressed, sintered and carbon-coated sepiolite pellet obtained with a press designed to prepare samples for infrared spectroscopy. Data collected were

processed with the Inca 200 Microanalysis Suite software. The weight% sum of oxides, showing no relevant heterogeneity, were properly averaged to obtain a reliable crystal-chemical formula.

Conventional XRPD data were collected on an automated Siemens D-5000 diffractometer in Bragg-Brentano geometry, using graphite monochromatized Cu-K α radiation and a zero-background flat sample holder.

Conventional thermogravimetric data were collected on relatively massive samples (ca. 15 mg) with a simultaneous TGA/DSC SDT Q600, TA Instruments, in N₂ flow with a heating rate of 10°C min⁻¹ from room temperature to 1000°C. DSC heat flow data were dynamically normalized using the instantaneous sample weight at any given temperature.

A state-of-the-art in-line coupled TGA–FTIR–GC–MS instrument from Perkin-Elmer was used to analyze the weight loss of both pristine and dye-conjugated sepiolite and the composition of the moieties released from the heated samples simultaneously.

TGA analysis: the high sensitivity (0.1 μ g) ultra-microbalance Pyris 1 from Perkin-Elmer was operated in N₂ flow (30 cm³ min⁻¹) at a heating rate of 15 °C min⁻¹ at the room temperature to 1000°C interval. A relatively large amount of sample (ca. 15 mg) was heated in every run to optimize the amount of gases released.

GC-MS analysis: the desorbed moieties were in-line conducted via a proprietary pressurized transfer line (Redshift, SrL – Vicenza, Italy) heated at 300 °C to a Clarus 500S gas chromatograph (Perkin-Elmer) with an integrated mass spectrometer as detector (Clarus 560S, Perkin Elmer). At a given time/temperature ca. 50 μ L of desorbed gas were injected into the GC system and a run performed automatically. The GC was operated with a standard nonpolar fused silica capillary column (DB5 MS) coated with a 5% diphenyl-dimethylpolysiloxane stationary phase. Total ion count (TIC) chromatograms were reported as well as some detailed mass spectra of specific chromatographic peaks.

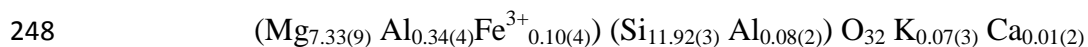
227

228

229 **3. Chemical analysis**

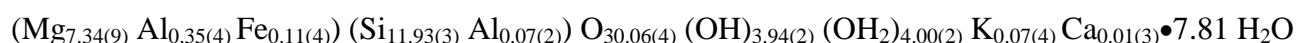
230 An accurate crystal-chemical formula for the studied sepiolite was obtained by means of SEM-
 231 EDS analyses. Such a procedure was adopted in order to check the consistency of the chemical
 232 formula provided by the supplier (Sigma-Aldrich: $\text{Mg}_2\text{H}_2\text{Si}_3\text{O}_9 \cdot x\text{H}_2\text{O}$), possible presence of
 233 exchangeable ions in the microchannels (Na, K, Ca), overall hydrous content and possible
 234 substitution of Mg with different ions (Al, Fe) in the octahedral sheet. This last aspect,
 235 interrelated to exchangeable ions content and overall electrical neutrality, may affect interatomic
 236 distances in the octahedral ribbons thus supplying useful information for crystallographic
 237 studies. Observations at high magnification (10K X) showed the fibrous habit of this sepiolite,
 238 formed by bundled aggregates of small fibres (Fig. 2) which individually present modest
 239 dimensions (3-4 μm long; 0.1 μm thick).

240 Chemical analyses, in the form of weight% of the different oxides, gave totals far from the ideal
 241 sum (100%) as a result of the high water content of the clay and, eventually, surface roughness
 242 of the analyzed pellet. Averaged analytical totals reached 85.6(6)%, the residual amount being
 243 consistent with the hydrous content of the mineral (Jones and Galan, 1988) whose loss is caused
 244 by both vacuum and exposure to the electron beam. Weight% of oxides measured for each
 245 analytical spot are listed in Table 1. All Fe was considered as Fe_2O_3 , though the presence of
 246 Fe^{2+} cannot be ruled out. The crystal-chemical formula, calculated on the basis of the
 247 dehydrated half unit cell (32 oxygens: Caillère and Hénin, 1972), is reported below:



249 Collected compositional data were also averaged and integrated with the experimentally found
 250 quantities of different kinds of water (zeolitic H_2O + structural OH_2 + framework $\text{OH} \cong 18.5$

wt%) as inferred from TGA (see below), in order to obtain an adequate estimate of the total hydrous content of the mineral. Despite the renowned difficulties in assigning the weight% losses to each water type and considering the discrepancies between such quantities and those resulting from the theoretical model (Caillère and Hénin, 1972), a recalculation of the EDS micro-analysis keeping into account H₂O, OH₂ and hydroxyls led to the following hydrated crystal-chemical formula:



Dehydrated and hydrated formulas are coherent with one another (differences encountered being within computed standard deviations) and both consistent with the ideal one. Though a typical Mg-rich clay [MgO: 24.2(4)%], quite a significant Al content [1.7(2)%, unstated by the supplier] was also detected. Recent studies, however (Garcia-Romero *et al.*, 2007; Garcia-Romero and Suárez, 2010), showed that analogous Al-rich sepiolites are not so uncommon. A very limited Si/Al substitution occurs also in tetrahedrons. Minor quantities of Fe³⁺ [Fe₂O₃: 0.7(3)%] also occupy octahedral sites. The sum of all octahedral cations (Mg + Al + Fe³⁺ = 7.80) is consistent with the theoretical value (8). The slight underestimate affecting the quantity of zeolitic H₂O (7.81) with respect to its ideal value (8) may be justified by the above mentioned difficulties in precisely attributing the water% resulting from TGA to the different kinds of water and is nevertheless contained within acceptable errors. In contrast structural OH₂ [4.00(2)], framework oxygen atoms [30.06(4)] and structural hydroxyls [3.94(2)] quantities are in excellent agreement with their theoretical values (4, 30 and 4, respectively). Furthermore, the quantity of exchangeable mono- and divalent cations in the channels (K, Ca) proved to be negligible [$\leq 0.3(1)\%$].

(INSERT FIGURE 2)

(INSERT TABLE 1)

275

276 4. Synthesis and stability

277

278 4.1. Synthesis

279 The preparation of the sepiolite + indigo pigment basically followed the procedure codified
280 in the literature for the laboratory synthesis of Maya Blue (Van Olphen, 1966; Kleber et al.,
281 1967; Sanchez Del Río et al., 2006; Polette-Niewold et al., 2007). This procedure consists of
282 three main steps:

283 i) Preparation of a dry mechanical mixture of sepiolite and indigo in proper quantities (2
284 wt%), ground until a homogeneous blue powder is obtained. The strong grinding itself
285 causes a variation in the hue of the powders, which gradually passes from a light to a
286 quite intense blue. As previously reported (Hubbard et al., 2003; Sanchez del Río et al.,
287 2006), such a colour change implies that sepiolite and indigo interact with one another –
288 at least at a certain extent – by merely crushing the powders even prior to the heating
289 process, probably as a result of a reduced grain size of the clay.

290 ii) Heating of the powders, dispersed on a wide glass surface in deionized water, up to
291 190°C for 20 hours. This step causes the hue to further vary, passing from a deep to a
292 slightly paler greenish blue.

293 iii) Purification of the pigment under a Soxhlet extractor in acetone (12 hours), with the aim
294 of removing the excess fraction of the dye not fixed to the sepiolite framework (Kleber et
295 al., 1967). The bluish hue of the exhausted solvent implies that a certain amount of
296 indigo, not sharply quantifiable, is washed away as testified also by a slight bleaching of
297 the powders.

298 4.2. Stability

The stability of the sepiolite + indigo (2 wt%) pigment was tested by means of chemical attacks at progressively increasing times with both acids and alkalis, in order to check possible colour variations and/or structural rearrangements. Obtained evidences were compared with those presented by an analogous palygorskite + indigo adduct, whose renowned resistance to acids and alkalis is well described in literature (Gettens, 1962; Van Olphen, 1966; Littmann, 1982; Sanchez del Río, 2006).

4.2.1. Acid attack

Acid attack was performed with concentrated HNO_3 (65%) at room temperature, which applied on pure indigo immediately decomposes its molecule into isatin ($\text{C}_8\text{H}_5\text{NO}_2$), a yellowish-red precipitate. Such an attack showed the more pronounced intrinsic fragility of the structure of sepiolite compared to that of palygorskite, as already reported by several authors (Myriam et al., 1998; Özdemir and Kipçak, 2004; Yebra-Rodríguez et al., 2003; Sanchez del Río et al., 2006; Kilislioglu and Aras, 2010). A prolonged acid treatment (4 days) almost completely destroyed the sepiolite lattice producing an amorphous phase, whereas an analogous treatment on palygorskite left the clay structure virtually unaltered (data not shown). The lower stability of sepiolite may be explained by the larger dimensions of its microtunnels, which undermine the solidity of the atomic packaging. Fixation of indigo in the sepiolite framework does not alter its vulnerability to prolonged HNO_3 attack: despite an apparent stability shown after a few minutes treatment, XRPD patterns collected at progressively increasing times (Fig. 3) show how the related diffraction maxima gradually tend to disappear as the structure was progressively dismantled. Visually, the prolonged HNO_3 attack caused the blue colour to gradually disappear in a few hours; after four days only a pale grayish powder remained. Analogous

treatments caused no appreciable difference, on the contrary, in both the colour and the structure of the palygorskite-based pigment (not shown).

(INSERT FIGURE 3)

4.2.2. Alkali attack

Concentrated NaOH (32%) was used for the alkali attack. Once again, the palygorskite + indigo pigment remained virtually unaffected after prolonged treatment, both in structure and in colour (data not shown). The sepiolite+indigo adduct, on the contrary, showed an unusual behavior: the blue hue of the compound tended to bleach slightly at progressively increasing times, but the clay structure was affected in a more peculiar way. A careful examination of XRPD patterns collected at increasing intervals (Fig. 4) shows how such treatment seems to induce a partial but progressive phase transition, which gradually turns sepiolite into a loughlinite-like phase, an analogous fibrous, pearly-white phyllosilicate with a silky luster but richer in Na (Fahey and Axelrod, 1948; Fahey et al., 1960). Loughlinite and sepiolite are virtually identical in appearance, both in hand specimen and microscopically. Though presenting similar XRPD patterns, the main difference is related to the d_{110} reflection which passes from 12.27 (sepiolite) to 12.90 Å (loughlinite – Fig. 4), as already stated by several authors (Echle, 1978; Serratosa, 1979; Van Olphen and Fripiat, 1979; Kadir et al., 2002). Recently Akyuz and Akyuz (2004) showed that FTIR spectroscopy can also be used, in addition to XRPD, to distinguish sepiolite from loughlinite as variations in both positions and intensities of selected OH and Si-O groups vibrational modes can be observed as a result of different structural morphology. The structure of loughlinite (ideal formula: $\text{Na}_2\text{Mg}_3\text{Si}_6\text{O}_{16} \cdot 8\text{H}_2\text{O}$), whose details have yet to be completely outlined, was first proposed by Preisinger (1963) and later discussed by Echle (1978). In loughlinite the marginal Mg ions

located at the borders of each TOT ribbon are substituted by two Na, one occupying the octahedral site and the other located in the channel and bonded to 6 H₂O molecules. As with sepiolite, loughlinite has the ability of selectively adsorbing polar and non-polar molecules on the external surfaces and/or in the channels (Akyuz and Akyuz, 2004, 2005, 2010; Akyuz et al., 2010).

Field observation and mineralogical determinations completed so far indicate that sepiolite and loughlinite, which may be found together in the same sedimentary unit, are both formed authigenically and independently in different natural physiochemical environments, rather than being the product of a transformation of one to the other (Kadir et al., 2002). In spite of this, it is acknowledged that the marked structural analogies between sepiolite and loughlinite allow their mutual phase transformation in controlled synthetic conditions to be feasible. Fahey et al. (1960) showed that water leaching of loughlinite in MgCl₂ solutions can cause transformation into sepiolite, allowing substitution of Na exchangeable ions with Mg. In addition, a phase transformation from sepiolite to loughlinite – similar to the one experimentally observed here, was previously described in the literature by Imai et al. (1969) who leached sepiolite with 6 N NaOH at 95°C for 1 hour or at room *T* for one day, thus obtaining a loughlinite-like phase. Subsequent treatment with an aqueous MgCl₂ solution caused the newly-formed synthetic loughlinite to convert back into sepiolite again. As stated above, formation of loughlinite was marked by an increase in the d_{110} spacing from 12.2 to 12.9 Å and no noticeable loss of crystallinity was observed (Imai et al., 1969; d’Espinose de la Caillerie and Friplat, 1992), in perfect agreement with the results presented here. The NaOH treatment, therefore, does not affect the lattice periodicity but causes a substitution of the edge octahedral Mg by two Na. Partially weathered synthetic loughlinite, where vacated octahedral positions are

filled with Na, may possess a higher cation exchange capacity (CEC) with respect to sepiolite, thus increasing the catalytic properties.

The XRPD pattern of the sepiolite + indigo (2 wt%) pigment bleached with NaOH at room *T* after 1 hour treatment shows that phase transformation of the hosting matrix to loughlinite was not complete, as only an intermediate enlarging of the d_{110} spacing can be observed (from 12.27 – pristine sepiolite – to 12.50 Å). After a 24 hours treatment, however, the shifting of the d_{110} basal reflection is complete (12.90 Å: Fig. 4 - magnification). This means that in the presence of indigo the gradual sepiolite/loughlinite phase transformation is not only favored but even accelerated, also without heating. A very prolonged treatment with NaOH (up to 6 days) caused no further shift in the basal d_{110} spacing but the sharper progressive appearance of several reflections at higher 2θ values, exclusively related to the presence of loughlinite (i.e peaks at 4.75, 3.60, 2.64 and 2.48 Å plus other minor features: Fahey et al., 1960 – Fig. 4). Curiously the very same alkali treatment (prolonged attack – 6 days – with concentrated NaOH) applied at room *T* on pristine sepiolite brought about no phase transformation to loughlinite, thus contradicting the results of the experiences of Imai et al. (1969) and D’Espinoose de la Caillerie and Friplat (1992). This could imply that presence of indigo might have a specific role in catalyzing such a process, although the importance of heating cannot be ruled out (i.e. an increase in temperature – 95°C – causes the phase transformation from sepiolite to loughlinite to be quicker: Imai et al., 1969; d’Espinoose de la Caillerie and Friplat, 1992).

The identity of the newly-formed mineral as a loughlinite-like phase is further supported by taking into account that a more drastic phase-transformation (i.e. from sepiolite into a laminar phyllosilicate, such as Na-saponite) would imply a severe

framework rearrangement by no means justifiable by the weak applied treatment (NaOH bleaching). In addition, the basal (d_{110}) reflection of saponites is usually higher, even before glycolation, than those typical of both sepiolite and loughlinite.

All observed evidence is therefore consistent with a phase transformation of the composite hosting matrix from sepiolite to loughlinite brought about as a result of concentrated NaOH bleaching. The exact role played by the guest indigo molecule in such process, however, may require further in-depth studies.

(INSERT FIGURE 4)

5. Thermogravimetric studies

Conventional thermograms (TGA)/derivative weight and heat flow (DSC)/derivative heat flow curves were recorded for both sepiolite and the sepiolite + indigo (2 wt%) pigment.

5.1. *Sepiolite*

The weight loss with increasing temperatures of the analyzed sepiolite (Fig. 5), though not consistently different from previous studies (Caillère and Hénin, 1957; Preisinger, 1959; Hayashi et al., 1969; Nagata et al., 1974; Rautureau and Mifsud, 1977; Ruiz et al., 1996; Weir et al., 2002; Hubbard et al., 2003; Ovarlez et al., 2006; Giulieri et al., 2009), deserves particular attention. As shown by the literature data, the TGA and derivative weight curves can be divided in three different regions, although the boundaries among them are not so sharp:

- i) In the low temperature region (room temperature – 280°C) a huge endothermic reaction (peaking upwards at $\cong 100$ -110°C in the derivative heat flow) testifies to the loss of superficially adsorbed water, together with the less severely bonded zeolitic H₂O. The

related total weight loss inferred from TGA is about 10.2%. A progressive, albeit less severe, decrease in weight proceeds as temperature rises. This involves both the residual, subordinate fraction of zeolitic H₂O (Serna et al., 1975), presumably related to molecules directly H-bonded to the structural OH₂ (Post et al., 2007), together with the loss of the first half of structural OH₂ (see below). This causes a further 3% weight loss, as shown by the 270°C peak in the derivative weight curve; associated reactions are still endothermic.

- ii) In the central region (280-630°C), structural OH₂ should be released by the clay framework. Such loss is expected to occur in two separate stages, each indicated by different endothermic reactions causing similar weight decreases (Jones and Galan, 1988): after the first half is lost, the structure folds to sepiolite-2H₂O; when the residual half has gone, “anhydrous” sepiolite is left (Post et al., 2007). In the studied sepiolite, however, the loss of the first half of the structural OH₂ is likely to occur in a broader but lower temperature range (200-330°C) with respect that reported in literature (327-350°), causing partial superposition of the related signals to the abovementioned occurring in the low temperature region. The related endothermic reaction in the derivative heat flow (Fig. 5) peaks at 220°C, with a further weak signal at 310°C. The already mentioned 270°C peak in the derivative weight has therefore to be related to the loss of residual zeolitic H₂O and first fraction of structural OH₂. Release of the second half of the structural OH₂, besides, is justified by presence in the derivative weight of a peak at 520°C, attesting a global weight loss of a further 2.8%; the related endothermic peak is hardly evident. Weight loss related to both derivative weight 270 and 520°C maxima is about 5.8%. Such an amount, though slightly higher than the value expected for the departure of structural OH₂ from the ideal formula (5.5%: Brauner and Preisinger, 1956), is consistent with the claimed additional presence of a residual zeolitic H₂O fraction.

iii) In the high temperature region ($> 630^{\circ}$) dehydroxylation occurs between 700 and 870°C , with the passage to clinoenstatite (Jones and Galan, 1988) or an amorphous phase (Lokanatha et al., 1985). In the derivative heat flow a huge endothermic peak appears at 830°C indicating loss of hydroxyl groups, immediately followed by an exothermic maximum at 840°C . The corresponding weight loss (2.5%), justified by a broad peak at 790°C in the derivative weight, is in good agreement with the theoretical amount (2.7%: Brauner and Preisinger, 1956). No further weight loss is observed at higher temperatures.

The global weight loss in the adopted temperature ramp, related to the release of different kinds of water (H_2O ; OH_2) and hydroxyls, amounts to 18.5%.

(INSERT FIGURE 5)

5.2. *Sepiolite + indigo (2 wt%) pigment*

A careful examination of the sepiolite + indigo composite thermogravimetric data (Fig. 6) shows subtle but significant differences when compared to pristine sepiolite. The pattern splitting in three different regions is even more uncertain.

i) In the low temperature region, the first endothermic reaction at $100\text{--}110^{\circ}\text{C}$ (loss of superficially adsorbed and most zeolitic H_2O) implies a lower weight loss (8.8%) with respect to that recorded for pure sepiolite (10.2%). Such a decrease (-1.4%), with all due probability related to a lower zeolitic H_2O amount leaving the clay matrix while heating, can be explained by indigo diffusion and partial occupation of the channels during the pigment synthesis. The observed evidence is consistent with Sanchez Del Rìo et al. (2009), who pointed out that only partial rehydration occurs in a palygorskite-based Maya Blue after heating, as a result of indigo encapsulation. A further weight loss, similar to that observed for pure sepiolite (3.3 %) proceeds until temperature reaches 320°C , as

shown by the presence of an analogous band in the derivative weight curve: such a peak, however, is not only slightly less pronounced than its counterpart above, but centered at a higher temperature (290 instead of 270°C). As the residual zeolitic H₂O and the first, loosely bound fraction of structural OH₂ are expected to be lost in such interval, it looks as if presence of indigo causes this latter fraction to bind more firmly to the clay framework. Related reactions are endothermic, evident maxima in the derivative heat flow peaking at 220 and 320°C.

- ii) In the central region (320-620°C) a further progressive weight loss is observed (3.3%). Such a decrease is not only slightly higher (2.8%) but shows a completely different trend with respect to that of pure sepiolite, as evidenced by comparing the related derivative weight profiles in the selected *T* interval. In particular, pure sepiolite shows an isolated band at 520°C whereas no well-defined derivative peak emerges for the sepiolite + indigo (2 wt%) pigment, but rather a slow and almost continuous weight loss distributed in the whole investigated temperature range. A more accurate examination reveals how such continuous weight decrease may approximately be divided in two broad but separate bands, the first approximately centered at 375 and the second at 520°C. While this latter component finds its natural attribution in the loss of the second half of structural OH₂, the former is accompanied by a broad endothermic peak visible at approximately 400°C in the derivative heat flow and may well be related to the release of indigo. Such attribution is consistent with the results of Hubbard et al. (2003) and Giulieri et al. (2009), who observed the presence of an analogous band in the DTG at \cong 350-360°C. Synchronized and sequential loss at progressively increasing temperatures of the indigo dye and the tightly-bound structural OH₂ implies possible existence of a mutual interaction between them, namely the first being encapsulated within sepiolite microchannels and presumably kept *in situ* by H-bonds donated by the second. It cannot be excluded, however, that the

release of both indigo and bound OH_2 may be homogeneously distributed in the analyzed T range rather than consequential, hence the above mentioned 375 and 520°C partially overlapped broad bands in the derivative weight being referred to both phenomena.

- iii) In the high temperature region no significant change occurs with respect to pure sepiolite: a slow but progressive weight loss occurs as dehydroxylation proceeds, causing a further 2.9% weight loss which is in excellent agreement with the value (2.7%) proposed by Brauner and Preisinger (1956). Variations in the derivative heat flow are absolutely analogous to those mentioned above.

The global weight loss in the adopted temperature ramp, related to the release of different kinds of water (H_2O ; OH_2), hydroxyls and adsorbed indigo molecules, is quite similar to that related to pristine sepiolite (18.3%).

(INSERT FIGURE 6)

6. Thermogravimetric analysis coupled with Gas-Chromatography (GC) and Mass Spectrometry (MS)

As stated above, conventional thermal studies showed thermograms of sepiolite (Fig. 5) and sepiolite + indigo (2 wt%) adduct (Fig. 6) to have slight but significant differences. In order to better investigate such divergences and specifically locate the temperature values at which indigo abandons the hosting framework, gas-chromatography and mass spectrometry were used to analyze the gaseous fraction expelled from the sepiolite-based Maya Blue during the heating ramp.

Fig. 7 is a straight comparison of both thermograms (dotted lines) and derivative weight curves (continuous lines) related to sepiolite (gray) and sepiolite + indigo (2 wt%) (black) in the 25-700°C region. It is evident that the main differences between the two samples are concentrated

in the 250-500°C interval. Vapour released from the sepiolite + indigo (2 wt%) specimen in three separate temperature values (330, 350 and 400°C, labeled A, B and C respectively in Fig. 7), marked by the most significant differences in the derivative weight compared to pristine sepiolite, were investigated with the abovementioned techniques in order to characterize the atomic and ionic species expelled from the pigment.

(INSERT FIGURE 7)

Collected gas chromatograms and mass spectra revealed significant evidence related to possible presence of indigo in all selected temperatures values. At 330°C the derivative weight patterns of both pristine sepiolite and sepiolite + indigo (2 wt%) show two sharp but different peaks (Fig. 7, A): while in the clay a more intense signal accounts for the loss of two different kinds of water (residual zeolitic H₂O and first half of structural OH₂); in the sepiolite-based Maya Blue the same peak is not only less intense but also slightly shifted towards higher temperatures. The gas chromatogram recorded for the vapors released by the sepiolite + indigo (2 wt%) adduct at 330° C (Fig. 8) shows several peaks collected in different times. Among these, a signal at about 13 min (marked by an asterisk in Fig. 8) can indisputably be related to presence of organic material compatible with the fragmentation path of indigo and indigo-derived moieties, according to what is reported in the NIST database. Such evidence is consistent with the corresponding mass spectrum (Fig. 9), in which appearance of three separate signals at 50, 76 and 104 m/z accounts for presence of gaseous organic fragments (C₄H₂, C₅H₂N/C₆H₄ and C₇H₄O respectively) in all probability resulting from fragmentation of the indigo molecule. Lack of detection in the mass spectrum of the molecular ion for the entire indigo molecule (M⁺ = 262 m/z) implies the solvated dye monomers may splinter into different organic fragments before being expelled from the hosting matrix due to progressive heating, rather than being ousted as a whole. Molecule fragmentation at temperatures nearing the dye sublimation point (ca. 300°C) further supports the possible existence of strong host/guest

interactions between indigo and the sepiolite framework, which may induce molecular strain thus favoring the onset of fractures in the adsorbed dye monomers.

Gas chromatograms recorded at higher temperatures (350 and 400°C; Fig. 8) show the persistence of the 13 min peak, though progressively diminished in intensity. Related mass spectra (not shown) remain consistent with the abovementioned results. This implies that the release of organic splinters derived from indigo fragmentation proceeds at higher temperatures too, though slightly diminished in quantity, thus justifying the slight weight loss recorded for the sepiolite + indigo (2 wt%) composite in the 350-450°C interval, where no appreciable weight loss occurs for pristine sepiolite (Fig. 7).

Observed evidence shows therefore that complete elimination of indigo adsorbed on the hosting sepiolite matrix is expected to start around 300°C and proceed until 500°C. Degradation and loss of the guest indigo dye due to progressive heating therefore partly begins at temperatures nearing its sublimation point (ca. 300°C). A subordinate fraction, however, appears to be more firmly anchored to the hosting framework, its departure occurring only at temperatures well above the dye sublimation point (\cong 500°C). As the departure of indigo covers the same temperature range related to loss of OH₂, it is legitimate to suppose that the host/guest interactions responsible for the composite stability may originate between the same components.

(INSERT FIGURE 8)

(INSERT FIGURE 9)

7. Concluding remarks

It is well known that a stable, Maya Blue-like composite can be synthesized by mixing and moderately heating (\leq 200°C) proper quantities of indigo with pure sepiolite, rather than palygorskite.

The chemical stability of such a pigment, however, is decreased with respect to a palygorskite-indigo based one, as partially pointed out also by previous studies (Sanchez Del Río et al., 2006; Doménech et al., 2009). The reasons might be found in the more pronounced intrinsic fragility of the crystal structure of sepiolite, compared to that of palygorskite, when attacked by both acids and alkalis. Such weakness is not likely to be modified as a consequence of the fixation of the dye molecule in the clay framework.

The partial phase transformation of the sepiolite + indigo (2 wt%) adduct into a loughlinite-based compound when attacked by NaOH, on the other hand, opens fascinating topics of discussion concerning the possible conversion of one clay to the other. Curiously, such a transformation is not likely to occur when bleaching pure sepiolite with NaOH. The role of indigo in this phase change, however, has yet to be understood. Further studies focused on the structural features of loughlinite (not definitely resolved so far) and the sites and possible interactions of indigo within the hosting framework may hopefully help to shed light on this aspect.

All collected evidence substantially confirm – though not always straightforwardly – the most quoted hypothesis postulated so far about the exact nature of the interactions existing between the sepiolite framework and indigo. Despite contrary claims, the dimensions of the dye (width: 4.8 Å) and the micro-pores (maximum effective width: 10.6 Å) are such that diffusion of the molecule inside the nano-tunnels is likely to be expected. Several authors (Ovarlez et al., 2006; Giulieri et al., 2009; Raya *et al.*, 2010) stated that the indigo chemisorptions in sepiolite occurs undoubtedly inside the channels. These results were recently confirmed by Giustetto et al. (2010), who in addition stated that indigo is linked to the sepiolite framework only on one side of its molecule, namely the one where its reactive groups (C=O and N–H) approach the border

of the channel. The other side of the molecule, left unrestrained in the tunnels, is presumably linked to the zeolitic H₂O molecules usually positioned there. This situation is apparently different from that of palygorskite, in which the narrower effective channel width (6.4 Å) allows chemical bonds to be formed on both sides of the guest indigo molecule. The clay/dye linkage is therefore stronger in a palygorskite-based rather than a sepiolite-based composite with indigo, due to the augmented number of possible bonds existing between the guest dye molecule and the hosting matrix. The lower stability of the sepiolite-based Maya Blue pigment, corroborated by the experimented stability tests, cannot therefore be exclusively ascribed to this clay's more enhanced structural fragility but also to its weaker interaction with the guest indigo dye.

TGA analysis gave indirect evidence about the presence of indigo inside the clay nano-tunnels, as the total amount of zeolitic H₂O lost while progressively heating the pigment was lower (8.8 wt%) than that measured from pure sepiolite (10.2 wt%). This implies that indigo is encapsulated inside the nano-tunnels, occupying volume that, by contrast, is filled by zeolitic H₂O in sepiolite. Both derivative weight and heat flow curves showed small but significant differences between pure sepiolite and the related composite with indigo in the 250-550°C temperature interval. While loss of OH₂ is likely to occur in two distinct steps for pure sepiolite (270 and 520°C respectively), the presence of indigo complicates such a situation as an almost continuous weight loss was observed, though with different intensities, between 290 and 550°C. Such loss has to be related to the sequential or contextual departure of both OH₂ and the guest dye molecules, possibly involved in mutual interactions.

Thermogravimetry combined with gas chromatography and mass spectrometry basically showed that departure from the composite matrix of organic splinters compatible with indigo fragmentation and Mg-coordinated OH₂ occurs concurrently in the same temperature interval (300-500°C), thus confirming that host/guest interactions are indeed established between these

two components. To form such interactions – presumably H-bonds between OH₂ and the dye donor and acceptor groups (N–H and C=O respectively), indigo is expected to diffuse inside the sepiolite channels or accommodate in the superficial grooves (half-channels) carving the surface of the clay fibres. It is legitimate to infer that the more conspicuous fraction of indigo leaving the hosting structure at more moderate temperatures ($\cong 300^{\circ}\text{C}$) could be related to molecules hosted in the superficial grooves or at the tip of the channels, whereas the subordinate residual dye fraction, whose loss occurs only at progressively higher temperatures (up to 500°C), could refer to molecules more deeply encapsulated within the channels and sheltered from the external environment.

To further investigate the structural features of the sepiolite + indigo (2 wt%) pigment and obtain further confirmation about the nature of the clay/dye interaction, a crystal structure refinement using the Rietveld method on synchrotron diffraction patterns has been performed. Hopefully, the related results will be published in the very near future (Giustetto et al., *subm.*).

All studies performed so far on the palygorskite/sepiolite adducts with indigo imply the possibility of synthesizing a new class of nanostructured compounds by exploiting the sorption properties of these clays. The potential fixation in both palygorskite and sepiolite matrices of differently colored dyes may lead to the creation of a new category of pigments, with all possible hues. Studies in the medical field proved that the fibrous habit of these clays is not dangerous for human health (Governa et al., 1995). An absence of poisonous materials (heavy-metals) and low production expenses would ensure, in addition, these pigments to be ecologically-oriented and cheap. Based on such premises, stimulating results were recently obtained in the synthesis of a palygorskite-based “Maya Red” pigment (Giustetto and Wahyudi, 2010).

Acknowledgments

The authors wish to thank Marco Travet, Dominique Scalarone and Roberto Cossio for their precious help in collecting thermo-gravimetric and SEM-EDS data respectively. We would like to thank Giacomo Chiari of the Getty Conservation Institute, Los Angeles, CA (USA), who first of all introduced us to the study of Maya Blue and for several years contributed his vast experience on the subject.

We also thank the referees of this paper (anonymous) and Editor Jock Churchman, who contributed with their precious advices to improve significantly the quality of the manuscript.

The TGA-FTIR-GC-MS measures have been obtained with the equipment acquired by the “G. Scansetti” Interdepartmental Center for Studies on Asbestos and Other Toxic Particulates, thanks to a grant by the Compagnia di San Paolo, Torino, Italy. IC is recipient of a post-doctoral fellowship from the Compagnia di San Paolo, Italy.

A special thank goes to Prof. Giovanni Ferraris, who helped with his support, suggestions and experience to significantly improve the results of this study.

References

- Akyuz, A., Akyuz, T., 2004. FT-IR spectra of natural loughlinite (Na-sepiolite) and adsorption of pyrimidine on loughlinite. *Journ. of Molecular Structure* 705 (1-3), 147-151.
- Akyuz, A., Akyuz, T., 2005. Study on the interaction of nicotinamide with sepiolite, loughlinite and palygorskite by IR spectroscopy. *Journ. of Molecular Structure* 744 (1-3), 47-52.
- Akyuz, A. Akyuz T., Akalin E., 2010. Adsorption of isoniazid onto sepiolite-palygorskite group of clays: an IR study. *Spectrochim. Acta A* 75, 1304-1307.
- Akyuz A., Akyuz T., 2010. Adsorption of 3- and 4-aminopyridine on loughlinite – An IR spectroscopic study. *Vibrational Spectroscopy* 53, 136-139.

- 674 Alkan, M., Demirbaş, Ö., Çelikçapa S., Dogan, M., 2004. Sorption of acid red 57 from aqueous solution onto
675 sepiolite, *J. Hazard. Mater. B* 116, 135–145.
- 676 Alkan, M., Demirbaş, Ö., Dogan, M., 2007. Adsorption kinetics and thermodynamics of an anionic dye onto
677 sepiolite. *Microporous and Mesoporous Materials* 101, 388–396.
- 678 Arnold, D. E., Branden, J.R., Williams, P.R., Feinman, G.M., Brown, J. P., 2008. The first direct evidence for the
679 production of Maya Blue: rediscovery of a technology. *Antiquity* 82, 151-164.
- 680 Bradley, W.F., 1940. Structure of attapulgite. *Amer. Mineral.* 25, 405-410.
- 681 Brauner, K., Preisinger, A., 1956. Structur und Entstehung des sepioliths. *Tschermaks Mineralogische und*
682 *Petrographische Mitteilungen* 6, 1-2.
- 683 Brühwiler, D., Calzaferri, G., Torres, T., Ramm, J.H., Gartmann, N., Dieu, L., Lòpez-Duarte, I., Martínez-Díaz,
684 M.V., 2009. Nanochannels for supramolecular organization of luminescent guests. *Journal of Materials*
685 *Chemistry* 19, 8040-8067.
- 686 Caillère, S., 1934. Analysis of palygorskite from Taodeni. *C.R. Acad. Sci., Paris* 198, 1795-1798.
- 687 Caillère, S., 1936. Nickeliferous sepiolite. *Bull. Soc. Franc. Minér.* 59, 163-326.
- 688 Caillère, S., Hénin, S., 1957. In: Mackenzie, R.C. (Ed.) *The differential thermal investigation of clays.*
689 *Mineralogical Society, London.*
- 690 Caillère, S., Hénin, S., 1972. Sepiolite. In: Brown, G. (Ed.) *The X-ray identification and crystal structures of clay*
691 *minerals. Mineralogical Society (Clay Minerals Group) London.*
- 692 Calzaferri, G., Huber, S., Maas, H., Minkowski, C., 2003. Host-guest antenna materials. *Angewandte Chemie Int.*
693 42, 3732-3758.
- 694 Càmara, F., Garvie, L.A.J., Devouard, B., Groy, T.L., Buseck, P.R., 2002. The structure of Mn-rich
695 taperssuatsiaite: A palygorskite-related mineral. *Amer. Mineral.* 87(10), 1458-1463.
- 696 Chiari, G., Giustetto, R., Ricchiardi, G., 2003. Crystal structure refinements of palygorskite and Maya blue from
697 molecular modelling and powder synchrotron diffraction. *Eur. Journ. of Mineral.* 15, 21-33.

- 698 Damyanova, S., Daza, L., Fierro, J.L.G., 1996. Surface and catalytic properties of lanthanum-promoted Ni/sepiolite
699 catalysts for styrene hydrogenation. *Journal of Catalysis* 159 (1), 150-161.
- 700 d'Espinose de la Caillerie, J.B., Friplat, J.J., 1992. Al modified sepiolite as catalyst or catalyst support. *Catalysis*
701 *Today* 14, 125-140.
- 702 De Yta, A., 1976. Análisis térmico diferencial sul Azul Maya. Tesis de Maestría p. 83.
- 703 Dogan, M., Ozdemir, Y., Alkan, M., 2007. Adsorption kinetics and mechanism of cationic methyl violet and
704 methylene blue dyes onto sepiolite. *Dyes and Pigments* 75 (3), 701–713.
- 705 Doménech, A., Doménech-Carbò, M.T., Sànchez del Rio, M., Vázquez de Agredos Pascual, M.L., 2009.
706 Comparative study of different indigo-clay Maya Blue-like systems using the voltammetry of microparticles
707 approach. *J. Solid State Electrochem.* 13, 869-878.
- 708 Echle, W., 1978. The transformations \leftrightarrow sepiolite-loughlinite: experiments and field observations. *Neues Jahrb.*
709 *Mineral., Abh.* 133, 303-321.
- 710 Fahey, J.J., Axelrod, J.M., 1948. Loughlinite, a new hydrous magnesium silicate. *Amer. Mineral.*, 33, 195.
- 711 Fahey, J.J., Ross, M., Axelrod, J.M., 1960. Loughlinite, a new hydrous sodium magnesium silicate. *Amer. Mineral.*
712 45, 270-281.
- 713 Ferraris, G., Khomyakov, A.P., Belluso, E., Soboleva, S.V., 1998. Kalifersite, a new alkaline silicate from Kola
714 Peninsula (Russia) based on a palygorskite-sepiolite polysomatic series. *Eur. Journ. of Mineral.* 10, 865-874.
- 715 Ferraris, G., Makovicky, E., Merlino, S., 2008. *Crystallography of modular materials*. Oxford, IUCr. Oxford
716 University Press.
- 717 Fois, E., Gamba, A., Tilocca, A., 2003. On the unusual stability of Maya Blue paint: molecular dynamics
718 simulations. *Microporous and Mesoporous Materials* 57, 263-272.
- 719 Garcia-Romero, E., Suárez, M., Santarén, J., Alvarez, A., 2007. Crystallochemical characterization of the
720 palygorskite and sepiolite from the Allou Kagne deposit, Senegal. *Clays and Clay Minerals* 55 (6), 606-617.
- 721 Garcia-Romero, E., Suárez, M., 2010. On the chemical composition of sepiolite and palygorskite. *Clays and Clay*
722 *Minerals* 58 (1), 1-20.

- 723 Gettens, R. J., 1962. Maya Blue: an unsolved problem in ancient pigments. *American Antiquity* 27, 557-564.
- 724 Giustetto, R., 2003. Studio strutturale sulla palygorskite e sul Maya Blue. PhD Thesis (unpublished), Università
725 degli Studi di Modena e Reggio Emilia, p. 183.
- 726 Giustetto, R., Llabres I Xamena, F., Ricchiardi, G., Bordiga, S., Damin, A., Chierotti, M., Gobetto, R., 2005. Maya
727 Blue: a computational and spectroscopic study. *J. Phys. Chem. B* 109 (41), 19360 -19368.
- 728 Giustetto, R., Levy, D., Chiari, G., 2006. Crystal structure refinement of Maya Blue pigment prepared with
729 deuterated indigo, using neutron powder diffraction. *Eur. Journ. of Mineral.* 18, 629–640.
- 730 Giustetto, R., Seenivasan, K., Bordiga, S., 2010. Spectroscopic characterization of a sepiolite-based Maya Blue
731 pigment. *Period. Mineral.* 79, 21-37.
- 732 Giustetto, R., Wahyudi, O., 2010. Sorption of red dyes on palygorskite: synthesis and stability of red/purple
733 Mayan nanocomposites. *Microporous and Mesoporous Materials*, DOI: 10.1016/j.micromeso.2010.12.004.
- 734 Giustetto, R., Levy, D., Wahyudi, O., Ricchiardi, G., Vitillo, J.. Crystal structure refinement of a sepiolite/indigo
735 Maya Blue pigment using molecular modeling and synchrotron diffraction. *Eur. Journ. of Mineral.* (submitted).
- 736 Glocker, E.F., 1847. *Generum et specierum mineralium secundum ordines naturales digestorium synopsis*. Halle,
737 348.
- 738 Governa, M., Valentino, M., Visonà, I., Monaco, F., Amati, M., Scancarello, G., Scansetti, G., 1995. In vitro
739 biological effects of clay minerals advised as substitutes for asbestos. *Cell. Biol. Toxic.* 11, 237-249.
- 740 Guggenheim, S., Eggleton, R.A., 1988. Crystal Chemistry, classification and identification of modulated layer
741 silicates. *Reviews in Mineralogy* 19, 675-725.
- 742 Hayashi, H., Otsuka, R., Imai, N., 1969. Infrared study of sepiolite and palygorskite on heating. *Amer. Mineral.* 54,
743 1613-1624.
- 744 Hubbard, B., Wenxing, K., Moser, A., Facey, G.A., Detellier, C., 2003. Structural study of Maya Blue: textural,
745 thermal and solid-state multinuclear magnetic resonance characterization of the palygorskite-indigo and
746 sepiolite-indigo adducts. *Clays and Clay Minerals* 51 (3), 318-326.
- 747 Imai, N., Otsuka, R., Nakamura, T., Koga, M., 1969. Artificial transformation of natural sepiolite into loughlinitite.
748 *Bull. Sci.Engr. Res. Lab., Waseda University* 46, 49-59.

- 749 Jones, B.F., Galan, E., 1988. Palygorskite and sepiolite. In: Bailey, S.W. (Ed.), *Hydrous Phyllosilicates – Reviews in*
750 *Mineralogy* 19, Mineralogical Society of America, Washington, 631-674.
- 751 Kadir, S., Bas, H., Karakas, Z., 2002. Origin of sepiolite and loughlinitite in a Neogene volcano-sedimentary
752 lacustrine environment, Mihaliççik-Eskisehir, Turkey. *Canad. Mineral.* 40, 1091-1102.
- 753 Kirwan, R., 1794. *Elements of Mineralogy* (2nd ed.). Elmsy, London. Vol. 1.
- 754 Kilislioglu, A., Aras, G., 2010. Adsorption of uranium from aqueous solution on heat and acid treated sepiolites.
755 *Appl. Radiat. Isot.* 10, 2016-2019.
- 756 Kleber, R., Masschelein-Kleiner, L., Thissen, J., 1967. Étude et identification du Bleu Maya. *Studies in*
757 *Conservation* 12, 41-55.
- 758 Littmann, E.R., 1982. Maya Blue further perspectives and the possible use of indigo as the colorant. *American*
759 *Antiquity* 47, 404-408.
- 760 Lokanatha, S., Mathur, B.K., Samantaray, B.K., Bhattacharjee, S., 1985. Dehydration and phase transformation in
761 sepiolite – a radial distribution analysis study. *Zeitsch. für Kristallographie* 171, 69-79.
- 762 Mackenzie, R.C., 1963. *De Natura Lutorum. Clays and Clay Minerals. Proceedings of the Eleventh National*
763 *Conference on Clays and Clay Minerals XI*, Pergamon Press, pp. 1–28.
- 764 Manciu, F.S., Ramirez, A., Durrer, W., Govani, J., Chianelli, R.R., 2008. Spectroscopic analysis of a dye-mineral
765 composite – a Raman and FT-IR study. *Journ. Of Raman Spectroscopy* 39, 1257-1261.
- 766 Martín, N., Melo, F., 2006. Mild hydrotreating over NiMo/sepiolite catalyst. *Reaction Kinetics and Catalysis*
767 *Letters* 88 (1), 35-41.
- 768 McCusker, L.B., 2005. IUPAC Nomenclature for ordered microporous and mesoporous materials and its
769 application to non-zeolite microporous mineral phases. *Reviews in Mineralogy and Geochemistry* 57, 1-16.
- 770 Merwin, H. E., 1931. Chemical analysis of pigments. In: Morris, E.H., Charlot, J. and Morris, A.A. (Eds.). *The*
771 *Temple of the Warriors at Chichen Itza, Yucatan, Washington D.C., Carnegie Institution of Washington,*
772 *Publication* 406.
- 773 Myriam, M., Suarez, M., Martin Pozas, J.M., 1998. Structural and textural modifications of palygorskite and
774 sepiolite under acid treatment. *Clays and Clay Minerals* 46, 225-231.

- 775 Nagata, H., Shimoda, S., Sudo, T., 1974. On dehydration of bound water of sepiolite. *Clays and Clay Minerals* 22,
776 285-293.
- 777 Nagy, B., Bradley, W.F., 1955. The structural scheme of sepiolite. *Amer. Mineral.* 40, 885-892.
- 778 O'Driscoll, M., 1992. European Cat Litter. Absorbing Market Growth. *Industrial Minerals* 299, 46.
- 779 Ovarlez, S., Chaze, A.M., Giulieri, F., Delamare, F., 2006. Indigo chemisorption in sepiolite. Application to Maya
780 Blue formation. *Comptes Rendu Chimie* 9, 1243-1248.
- 781 Ovarlez, F., Giulieri*, S., Chaze, A.M., Delamare, F., Raya, J., Hirschinger, J., 2009. The incorporation of indigo
782 molecules in sepiolite tunnels. *Chem. Eur. J.* 15, 11326-11332.
- 783 Özdemir, M., Kipçak, I., 2004. Dissolution kinetics of sepiolite in hydrochloric acid and nitric acid. *Clays and*
784 *Clay Minerals* 52, 714-720.
- 785 Özdemir, Y., Doğan, M., Alkan, M., 2006. Adsorption of cationic dyes from aqueous solutions by sepiolite.
786 *Microporous and Mesoporous Materials* 96 (1–3), 419–427.
- 787 Perrault, G., Harvey Y., Pertsowsky R., 1975. La yofortierite, un nouveau silicate hydraté de manganèse de St.
788 Hilaire, P.Q. *Canad. Mineral.* 13, 68-74.
- 789 Polette-Niewold, L.A., Manciu, F.S., Torres, B., Alvarado Jr., M., Chianelli, R.R., 2007. Organic/inorganic
790 complex pigments: Ancient colors Maya Blue. *Journ. Of Inorg. Biochem.* 101, 1958-1973.
- 791 Post, J.E., Bish D.L., Heaney P.J., 2007. Synchrotron powder X-ray diffraction study of the structure and
792 dehydration behavior of sepiolite. *Amer. Mineral.* 92, 91-97.
- 793 Preisinger, A., 1959. X-ray study of the structure of sepiolite. *Clays and Clay Minerals* 6, 61-67.
- 794 Preisinger, A., 1963. Sepiolite and related compounds: its stability and application. *Proceedings of the Tenth*
795 *National Conference on Clays and Clay Minerals*, Pergamon Press, pp. 365-371.
- 796 Rautureau, M., Mifsud, A., 1977. Etude par microscope electronique des differents etats d'hydratation de la
797 sepiolite. *Clay Minerals* 12, 309-318.

- 798 Raya, J., Hirschinger, J., Ovarlez, S., Giulieri, F., Chaze, A.M., Delamare, F., 2010. Insertion of indigo molecules
799 in the sepiolite structure as evidenced by $^1\text{H} - ^{29}\text{Si}$ heteronuclear correlation spectroscopy. *Physical Chemistry*
800 *Chemical Physics* 12 (43), 14508-14514.
- 801 Reinen, D., Köhl, P., Muller, C., 2004. Colour centres in 'Maya Blue' – the incorporation of organic pigment
802 molecules into the palygorskite lattice. *Z. Anorg. Allg. Chem.* 630, 97-103.
- 803 Reyes-Valerio, C., 1993. *De Bonampak al Templo Mayor: el Azul Maya en Mesoamerica*. Siglo XXI Editores.
- 804 Ruiz, R., del Moral, J.C., Pesquera, C., Benito, I., González, F., 1996. Reversible folding in sepiolite: study by
805 thermal and textural analysis. *Thermochimica Acta* 279, 103-110.
- 806 Rytwo, G., Nir, S., Crespin, M., Margulies, L., 2000. Adsorption and interactions of methyl green with
807 montmorillonite and sepiolite. *Journal of Colloid and Interface Science* 222 (1), 12.
- 808 Sanchez Del Río, M., Martinetto, P., Reyes-Valerio, C., Dooryhée, E., Suárez, M., 2006. Synthesis and acid
809 resistance of Maya Blue pigment. *Archaeometry* 48 (1), 115-130.
- 810 Sanchez Del Rio, M., Boccaleri, E., Milanesio, M., Croce, G., Van Beek, W., Tsiantos, C., Chrysikos, D., Gionis,
811 V., Kacandes, G.H., Suarez, M., Garcia-Romero, E., 2009. A combined synchrotron powder diffraction and
812 vibrational study of the thermal treatment of palygorskite-indigo to produce Maya Blue. *J. Mater. Sci.* 44,
813 5524-5536.
- 814 Serna, C., Ahlrichs, J.L., Serratos, J.M., 1975. Folding in sepiolite crystals. *Clays and Clay Minerals* 23, 452-457.
- 815 Serratos, J.M., 1979. In: M.M. Mortland, V.C. Farmer (Eds.), *Proceedings of 6th International Clay Conference*,
816 Elsevier, Amsterdam, pp. 99-109.
- 817 Shariatmadari H, Mermut, A.R., Benke, M.B., 1999. Sorption of selected cationic and neutral organic molecules on
818 palygorskite and sepiolite. *Clays and Clay Minerals* 47, 44-53.
- 819 Shimizu, K., Rei, M., Shin-ichi, K., Tatsuya, K., Yoshie, K., 2004. Pd-sepiolite catalyst for Suzuki coupling
820 reaction in water: Structural and catalytic investigations. *Journ. Of Catalysis* 227 (1), 202-209.
- 821 Springer, G., 1976. Falcondoite, nickel analogue of sepiolite. *Canad. Mineral.* 14, 407-409.
- 822 Van Olphen, H., 1966. Maya Blue: a clay-organic pigment?. *Science* 154, 645-646.

- 823 Van Olphen, H, Fripiat, J.J., 1979. Data handbook for clay minerals and other non-metallic minerals, Pergamon
824 Press, New York, p. 184.
- 825 Yebra-Rodríguez, A., Martín-Ramos, J.D., del Rey, F., Viseras, C., Lòpez-Galindo, A., 2003. Effect of acid
826 treatment on the structure of sepiolite. *Clay Minerals* 38, 353-360.
- 827 Weir, M.R., Kuang, W., Facey, G.A., Detellier, C., 2002. Solid-state nuclear magnetic resonance study of sepiolite
828 and partially dehydrated sepiolite. *Clays and Clay Minerals* 50, 240-247.
- 829
- 830
- 831
- 832
- 833
- 834
- 835
- 836
- 837
- 838
- 839
- 840
- 841
- 842
- 843

Table captions

Table 1. Chemical composition of the studied sepiolite measured by SEM-EDS on individual analytical spots. Last column lists the averaged values for all oxides.

Oxides (wt %)	Sepiolite										Average
	1	2	3	4	5	6	7	8	9	10	
MgO	24.16	24.30	23.38	23.66	24.33	24.47	24.31	24.03	24.52	24.64	24.2(4)
Al ₂ O ₃	1.70	1.67	2.13	1.91	1.72	1.61	1.64	1.64	1.79	1.58	1.7(2)
SiO ₂	58.96	58.52	58.19	58.43	58.70	58.81	58.77	58.02	58.84	59.18	58.6(4)
Fe ₂ O ₃	0.75	0.57	0.96	0.96	0.81	0.71	0.00	0.64	0.78	0.71	0.7(3)
K ₂ O	0.34	0.22	0.39	0.42	0.25	0.00	0.34	0.28	0.32	0.24	0.3(1)
CaO	0.00	0.00	0.00	0.00	0.00	0.00	0.00	0.00	0.40	0.00	0.0(1)
Total	85.91	85.28	85.05	85.38	85.81	85.60	85.06	84.61	86.65	86.35	85.6(6)

Table 1.

Figure captions

Figure 1. The structure of sepiolite (taken by Post et al., 2007). The chessboard-like disposition of interconnected TOT ribbons causes the framework to be crossed by large nano-tunnels (maximum effective width: 10.6 Å) along *z*, filled by weakly-bound zeolitic H₂O (not shown for clarity). Unit cell is evidenced by continuous lines.

Figure 2. The fibrous habit of the studied sepiolite observed on SEM (secondary electrons, 10K magnification).

Figure 3. XRPD patterns of sepiolite + indigo (2 wt%) pigment attacked with concentrated HNO₃ (65%) at progressively increasing times. The diffraction maxima show reduced intensities until almost complete disappearance after a 4 days period, as a result of the gradual destruction of the clay crystal structure. Diffractograms were shifted on the Y axis for sake of clarity.

Figure 4. XRPD patterns of sepiolite + indigo (2 wt%) pigment attacked at progressively increasing times with concentrated NaOH (32%). Rather than disappearing, the diffraction maxima show shifts in their positions implying that a phase change (from sepiolite to loughlinite) is likely to occur. The most pronounced shift concerns the (110) peak (magnified in the upper right corner). Diffractograms were shifted on the Y axis for sake of clarity.

Figure 5. Observed TGA/derivative weight and heat flow/derivative heat flow curves for sepiolite. Vertical scale for the TGA curve is weight loss%.

Figure 6. Observed TGA/derivative weight and heat flow/derivative heat flow curves for the sepiolite + indigo (2wt%) pigment. Vertical scale for the TGA curve is weight loss%.

Figure 7. Thermograms (dotted lines) and weight derivative (continuous line) of sepiolite (gray) and sepiolite + indigo (2 wt%) (black) in the 25-700°C region.

Figure 8. Gas chromatograms of the vapour released from the sepiolite + indigo (2 wt%) composite at 330, 350 and 400°C.

Figure 9. Mass spectrum of the moieties eluted by the sepiolite + indigo (2 wt%) composite at about 13 min at 330°C (peak marked by an asterisk in Fig. 8): m/z 50 \Rightarrow C_4H_2 ; m/z 76 \Rightarrow C_5H_2N/C_6H_4 ; m/z 104 \Rightarrow C_7H_4O .